



Article

A More Drought Resistant Stem Xylem of Southern Highbush Than Rabbiteye Blueberry Is Linked to Its Anatomy

Ya Zhang ^{1,*}, Jia-Bao Liu ^{2,†} and Xi-Xi Zhang ¹

¹ Anhui Provincial Key Laboratory of the Conservation and Exploitation of Biological Resources, College of Life Sciences, Anhui Normal University, Wuhu 241000, China; qqqqqq@ahnu.edu.cn

² College of Ecology and Environment, Anhui Normal University, Wuhu 241000, China; liujiabao@ahnu.edu.cn

* Correspondence: zhangya@ahnu.edu.cn

† These authors contributed equally to this work.

Abstract: Increasing extreme drought events due to climate change may cause severe damage to blueberry industries, including decreased fruit yield and quality. Previous studies on drought tolerance of blueberries focus mainly on functional changes of leaves, while hydraulic properties of blueberry stems related to drought resistance are poorly reported. Here, both xylem anatomical and functional traits of stems of two southern highbush (SHB) and three rabbiteye blueberry (REB) cultivars were investigated. Compared with REB, SHB showed lower sapwood hydraulic conductivity (K_S) and P_{50} (xylem water potential with 50% embolism in xylem), suggesting that SHB has less conductive but safer xylem than REB. The hydraulic functional differences between two blueberry xylems were highly related to their significant differences in vessel anatomy. Small vessel diameter and total inner pit aperture area per vessel area (A_{PA}) limited the hydraulic conductivity of SHB xylem, but high conduit wall reinforcement, wood density, and vessel-grouping index in SHB xylem showed strong mechanical support and safe water transport. Besides, pseudo-tori pit membranes were found in all five cultivars, while the similar thickness of homogenous pit membrane in two blueberry species was not linked to other functional traits, which may be due to its limited measurements. These results reveal a trade-off between the water transport efficiency and safety in the blueberry xylem and clarify the variance of stem drought resistance in different cultivars from a hydraulic perspective. Further studies with such a perspective on other organs of blueberries are required to understand the drought tolerance of a whole plant, which builds a solid foundation for the introduction, cultivation, and management of blueberry industries.



Citation: Zhang, Y.; Liu, J.-B.; Zhang, X.-X. A More Drought Resistant Stem Xylem of Southern Highbush Than Rabbiteye Blueberry Is Linked to Its Anatomy. *Agronomy* **2022**, *12*, 1244. <https://doi.org/10.3390/agronomy12051244>

Academic Editors: Pirjo Mäkelä, Mercè Llugany, Peter A. Roussos and Mumtaz Cheema

Received: 13 April 2022

Accepted: 21 May 2022

Published: 23 May 2022

Publisher's Note: MDPI stays neutral with regard to jurisdictional claims in published maps and institutional affiliations.



Copyright: © 2022 by the authors. Licensee MDPI, Basel, Switzerland. This article is an open access article distributed under the terms and conditions of the Creative Commons Attribution (CC BY) license (<https://creativecommons.org/licenses/by/4.0/>).

Keywords: embolism resistance; drought adaptability; xylem anatomy; *Vaccinium corymbosum*; *Vaccinium ashei*

1. Introduction

Blueberries are common names for a variety of *Vaccinium* species belonging to Ericaceae. Due to their high nutritional and economic value, blueberries have become an important fruit tree in many countries, such as America, Chile, and China [1]. The major worldwide cultivated blueberry species include lowbush blueberry (*Vaccinium angustifolium* Ait.), rabbiteye blueberry (*Vaccinium ashei* Reade), and highbush blueberry (*Vaccinium corymbosum* L.). Highbush blueberries are further separated into northern, southern, and intermediate type depending on their chilling requirements and winter hardness [2]. In general, southern highbush (SHB) and rabbiteye blueberries (REB) require fewer chilling hours and are less tolerable to winter temperatures much below freezing than the other blueberries [2]. Therefore, SHB and REB have been introduced largely to warmer and hotter regions, which may suggest their adaptability to arid environments. However, blueberries normally have a shallow root system and restricted lateral roots, which limit their cultivation in arid regions [3,4]. Besides, extreme drought events can lead to severe problems for the blueberry industry, such as reduced yields, impaired fruit quality, and

increased irrigation costs [5,6]. The drought tolerance of blueberries, therefore, has become an issue of concern, which is important for blueberry introduction and management.

Previous studies on drought tolerance of blueberries mostly focused on the physiological and molecular changes of plants, especially in leaves, under drought conditions [7,8]. Drought stress was found to cause a significant decrease in photosynthesis rate, gas exchange, photochemical efficiency of photosystem II (Fv/Fm), relative water content, chlorophyll, and carotenoid content in different highbush blueberry cultivars [7–11]. Meanwhile, proline and exogenous spermidine could alleviate the negative effect of water deficit in blueberry leaves [7,11]. Besides, arbuscular mycorrhizal fungi inoculation in roots of blueberries could maintain a greater abundance of differentially abundant proteins (DAPs) under drought stress, which may contribute to plant drought tolerance altering amino acid metabolism and signal transduction [4]. However, understanding the drought tolerance of blueberries from xylem hydraulic properties is poorly reported.

Xylem, featured in vessels, is the most important pathway for long-distance water transport in angiosperms. However, when drought events occur, gas dissolved in xylem sap may expand and grow into an embolism with increasing tension in the xylem. These embolisms, induced by drought, could block functional vessels, interrupt the continuous water flow, and impair the water supply for the whole plant [12,13]. The xylem embolism vulnerability curve, introduced by Tyree and Sperry [14], is commonly used to estimate the xylem embolism resistance in plant physiology. It reveals the relationship between the xylem water potential (i.e., the drought degree in xylem) and the percentage of embolism occurring in the xylem (normally represented by the percent loss of hydraulic conductivity). Since the water flow and embolism spreading in the xylem share the same pathway (i.e., pits, which are mainly openings on the lateral vessel walls), the xylem anatomical traits of a certain species largely affect its hydraulic properties and drought tolerance. In general, species adapted to arid regions are prone to low conductivity xylem with small vessels, few pit numbers, and thick pit membranes [15–18].

However, the structural and functional traits of blueberry xylem related to its drought resistance are poorly surveyed. The stem vulnerability curve of Bluecrop (a highbush blueberry cultivar) was reported by Améglio et al. [19], but a linking of the hydraulic functions and anatomical features of stem xylem is lacking. Here, xylem anatomical and functional traits in stems of SHB and REB, including five cultivars, are investigated to explain their potential difference in drought tolerance. Relationships among multiple structural and functional traits linked to xylem drought resistance are also surveyed. We hypothesize that (1) stem xylems of SHB and REB show different embolism resistance and (2) drought resistance of stem xylem in five blueberry cultivars is linked to their xylem anatomy. This study will provide a new perspective for understanding the drought adaptability of different blueberries and offer some scientific bases for the introduction, garden management, and water irrigation of blueberries.

2. Materials and Methods

2.1. Plant Materials

Two blueberry species, including five cultivars growing at Huiwang Meiling Blueberry Plantation in Wuhu, China (118°23′2.4″ E, 30°51′3.59″ N, 88 m), were selected in this study; they were: *Vaccinium corymbosum* (Southern highbush, including O’Neal and Misty) and *Vaccinium ashei* (Rabbiteye, including Britewell, Tifblue, and Climax). Several healthy individuals of each cultivar were selected for sample collection from July to October in 2020 and 2021. During this period, all cultivars were at the post-fruit stage. The one-year branches of five different cultivars were collected. A list of xylem functional and anatomical traits measured in this study is given in Table 1.

Table 1. List of traits included in the study with abbreviations, definitions, and units.

| Abbreviation | Definition | Unit |
|--------------------------|---|--|
| P_{12}, P_{50}, P_{88} | Xylem water potential at 12, 50, and 88% loss of hydraulic conductivity | MPa |
| K_H | Branch hydraulic conductivity | $\text{kg m s}^{-1} \text{MPa}^{-1}$ |
| K_S | Sapwood hydraulic conductivity | $\text{kg s}^{-1} \text{MPa}^{-1} \text{m}^{-1}$ |
| D_V | Vessel diameter | μm |
| VD | Vessel density | No. mm^{-2} |
| CWR | Conduit wall reinforcement | / |
| WD | Wood density | g cm^{-3} |
| VG | Vessel-grouping index | / |
| PD | Pit density | $\text{No. } \mu\text{m}^{-2}$ |
| A_{SP} | Area of single pit aperture | μm^2 |
| A_{PA} | Total inner pit aperture surface area per vessel area | mm^2 |
| T_{PM} | Intervessel pit membrane thickness | nm |

Note: / indicates that the calculated value for the trait has no unit and represents a number only.

2.2. Stem Hydraulic Conductivity

According to Sperry et al. [20], stem hydraulic conductivity (K_H , $\text{kg m s}^{-1} \text{MPa}^{-1}$) was measured for five cultivars. Briefly, three branches of each cultivar, which were longer than the maximum vessel length based on the gas injection method [21], were sampled in the early morning. Branches were immediately put underwater, covered with a black plastic bag to prevent evaporation, and transferred to laboratory within 2 h. Branches were trimmed into 60 cm long segments underwater, leaves were cut, and glue (AALOCTLTE AA401, Zhenkunxing Office Supplies Store, Dongguan, China) was applied to the cut surface. Then, branch segments were connected to a modified Sperry apparatus for hydraulic conductivity measurements. Briefly, the distal end of the segment was connected to a 60 cm high water column (10 mM KCl solution) and the other end to a pipette. The flow rate (F , $\mu\text{g s}^{-1}$) was determined by the time taken by water running through a 0.01 mL in the pipette. The hydraulic conductivity of the segment (K_H , $\text{kg m s}^{-1} \text{MPa}^{-1}$) was then calculated as:

$$K_H = F/(P/L), \quad (1)$$

where P represents the pressure applied to the segment (i.e., 0.006 MPa) and L represents the length of the segment. The sapwood area of the segment at the base was determined with 1% safranin dye, and the sapwood hydraulic conductivity (K_S , $\text{kg s}^{-1} \text{MPa}^{-1} \text{m}^{-1}$) was calculated as the hydraulic conductivity divided by the sapwood area.

2.3. Vulnerability Curves

The bench dehydration method [20] was applied to determine the embolism vulnerability curves of five cultivars. Branches of each cultivar were sampled in the early morning and then transferred to the laboratory in a water-filled basket and covered with a black plastic bag. The branches were placed on the experimental table to dry naturally from 0 h to several days to obtain a tension gradient in the xylem. Then, branches were completely wrapped with a black plastic bag for at least 1 h to reach water equilibrium between the leaves and stem. Three leaves from different positions of each branch were cut to measure the water potentials with a pressure chamber (PMS 1505EXP, Corvallis, OR, USA), and the average value was taken as the xylem water potential of the branch (Ψ , MPa). Branches were then put underwater for 1 h to release the tension, trimmed into 20 cm long segments, and connected to the Sperry apparatus as described before. The initial hydraulic conductivity (K_i , $\text{kg m s}^{-1} \text{MPa}^{-1}$) of each segment was measured first. The branch segment was then flushed with 10 mM KCl solution via the pressure chamber under 0.2 MPa for 30 min to remove the xylem embolism. The maximum hydraulic conductivity

(K_{max} , $\text{kg m s}^{-1} \text{MPa}^{-1}$) was measured, and the percentage loss of hydraulic conductivity (PLC, %) of each segment was calculated as:

$$\text{PLC} = 100 \times (K_{max} - K_i) / K_{max} \quad (2)$$

The xylem vulnerability curve was then established by plotting different xylem water potentials against PLC values using the equation:

$$\text{PLC} = 100 / (1 + \exp(S/25) / (\Psi - b)), \quad (3)$$

where S represents the slope of the fitted curve, and b is the xylem water potential when the xylem hydraulic conductivity loss is 50% (P_{50} , MPa).

Then, P_{12} (MPa) and P_{88} (MPa), i.e., the xylem water potential at 12% and 88% loss of xylem hydraulic conductivity, were calculated [22] as:

$$P_{12} = 2 / (S/25) + b, \quad (4)$$

$$P_{88} = -2 / (S/25) + b, \quad (5)$$

where the S and b values were obtained from Equation (3). The value of P_{12} represented the beginning of embolism occurring in the xylem, and P_{88} represented the severe embolism in the xylem, which was irreversible.

2.4. Wood Density

After the hydraulic measurements of the branches, three 3–5 cm long segments with bark and piths removed were cut from different positions to measure the wood density, and the average value was taken to represent the wood density of the branches. The wood density was calculated as the ratio of the dry weight to the fresh volume of the sapwood. The dry weight of the sapwood was obtained by putting the sapwood in an oven at 70 °C for 48 h. The volume of fresh sapwood was taken as the water volume using the water replacement method.

2.5. Light Microscopy (LM)

Several 1–2 cm long branch segments of each cultivar stored in FAA fixative were chosen for the wood anatomy. Segments were sectioned using a microtome (Leica RM2016, Shanghai, China) to obtain multiple cross-sections with a 20 μm thickness. Sections were dyed for 5–10 min with 1% safranin and 0.5% astra blue mixed dye solution, cleaned with water, and dehydrated with a gradient ethanol solution (50%, 70%, 85%, 95%, and 100%) for 1 min. Then, sections were transferred to a slide and covered with a drop of neutral resin to make a permanent slice. The xylem structure of each cultivar was observed and photographed under a light microscope (DMi8, Leica, Wetzlar, Germany) for further measurements of multiple traits of the xylem (see definitions and abbreviations in Table 1). Vessel diameter (D_V , μm) was averaged from two measurements at different axes. Vessel density (VD, No. mm^{-2}) was calculated as the number of vessels in a selected area of the xylem. Vessel-grouping index (VG) was calculated as the ratio of the total number of vessels to the total number of vessel groupings in a selected area of xylem, where a solitary vessel was also defined as a vessel-group. The conduit wall reinforcement (CWR), which indicated theoretical vessel implosion resistance, was calculated as the square of the ratio of vessel wall thickness to D_V . For each cultivar, D_V was measured based on at least 100 vessels, while VD and VG were measured based on at least 18 measurements and 50 vessel groups, respectively. All minimum measurement requirements were based on Scholz et al. [23].

2.6. Scanning Electron Microscopy (SEM)

Several 0.5–1 cm long branch segments of each cultivar were selected and cut into ca. 1 mm thick radial sections using sharp blades. These sections were dried on the bench at

room temperature for 5 days, fixed on a sample stage by the conductive tape, and sputter-coated with gold-palladium (Kyky sbc-12, KYKY Technology Co., Beijing, China) for 1 min with a 15 mA current. Samples were then observed and photographed under a scanning electronic microscope (JSM-6390LV, JEOL Ltd., Tokyo, Japan) with 10 kV voltage. The pit density (PD, No. μm^{-2}) and the single pit aperture area (A_{SP} , μm^2) were measured based on at least 20 measurements. The total inner pit aperture area per vessel area (A_{PA} , mm^2) was defined according to Wheeler et al. [24], which was calculated as follows:

$$A_{PA} = \pi \times \left(\frac{\sum D_V^4}{N} \right)^{\frac{1}{4}} \times L_V \times \text{Fpf} \times \frac{\sum L_{VW}}{\sum P_V} \quad (6)$$

where Fpf represents pit field fraction calculated as the ratio of the total area of inner pit aperture in a selected area to the selected area on vessel lateral walls. Other parameters in this equation were based on measurements in xylem cross-sections. For example, D_V represented the vessel diameter, N represented the number of vessels included in a selected xylem area, L_{VW} was the length of the vessel wall contact between adjacent vessels, P_V was the vessel perimeter, and L_V represented the vessel length obtained by the silicone injection method [25].

2.7. Transmission Electron Microscopy (TEM)

Several fresh 0.5–1 cm long segments of each cultivar with bark removed were selected and stored in water to avoid pit membrane shrinkage [26,27]. Then, 1–2 mm^3 xylem cubes were cut with sharp blades underwater and put in a fixative solution (2.5% glutaraldehyde solution, 0.1 M phosphate buffer, 1% sucrose solution, pH 7.3) in a refrigerator for 24 h. Samples were then washed 3–4 times with 0.1 M phosphate buffer, stained with 1% osmium tetroxide (mixed with 0.1 M phosphate buffer) at 20 °C for 2 h, and washed 3 times again with 0.1 M phosphate buffer. Then, samples were dehydrated in a gradient ethanol solution (30%, 50%, 70%, 80%, 85%, 90%, 95%, 100%, 100%) for 15 min and embedded in acetone with a rising amount of epoxy resin (2:1, 1:1, 1:2) and pure epoxy resin at 37 °C for 8 h. Samples in resin were polymerized in an oven at 60 °C for 48 h and sectioned on an ultra-microtome (EMUC7, Leica, Wetzlar, Germany). Ultra-thin sections with an 80–100 nm thickness were then dyed with 2% saturated aqueous solution of uranyl acetate and lead citrate for 15 min. Then, sections were dried at room temperature overnight, fixed on copper mesh, and observed under a transmission electron microscope at 80 kV accelerating voltage (HT7700, Hitachi, Tokyo, Japan). TEM images were used to determine the pit membrane thickness of each cultivar, averaged from measurements at the center and pit annulus (i.e., close to the pit border). In general, pit membrane thickness was taken from at least 7 measurements.

2.8. Statistics

ImageJ software (version 1.50i, National Institutes of Health, Bethesda, MD, USA) was used for all anatomical measurements on LM, SEM, and TEM images. SPSS 20.0 (SPSS Inc., Chicago, IL, USA) was used for statistical analysis to analyze the data at the interspecific level and inter-cultivar level. Kolmogorov–Smirnov test was applied first to justify the normality of the data. If data were normally distributed, statistical analysis was performed using the ANOVA test with 5% as the level of significance. If data were not normally distributed, a non-parametric test was applied. Correlations among xylem structural and functional traits were analyzed using Pearson's correlation. SigmaPlot 14.0 (Systat Software Inc., Düsseldorf, Germany) was used to make graphs.

3. Results

3.1. Differences in Xylem Functional Traits

All vulnerability curves of five blueberry cultivars showed an “S” shape (Figure 1). Embolism vulnerability of rabbiteye blueberry (REB) branches, represented by the P_{50} values, was higher than that of southern highbush blueberry (SHB), although a statistical

significance was lacking ($p = 0.87$). Given the low P_{50} value referring to high embolism resistance, the order of xylem embolism resistance ability of five blueberry cultivars from strong to weak was: O'Neal > Misty > Tifblue > Britewell > Climax (Figure 1; Table S1), where O'Neal showed the lowest P_{50} (−1.70 MPa) and Climax showed the highest P_{50} (−1.36 MPa). Tifblue had the most sensitive air-entry point ($P_{12} = -0.07$ MPa), and Misty was the least sensitive ($P_{12} = -0.58$ MPa). Similar to the trend of P_{50} values, O'Neal had the strongest ultimate tolerance ($P_{88} = -3.08$ MPa), and Climax showed the weakest ultimate tolerance ($P_{88} = -2.30$ MPa) (Table S1).

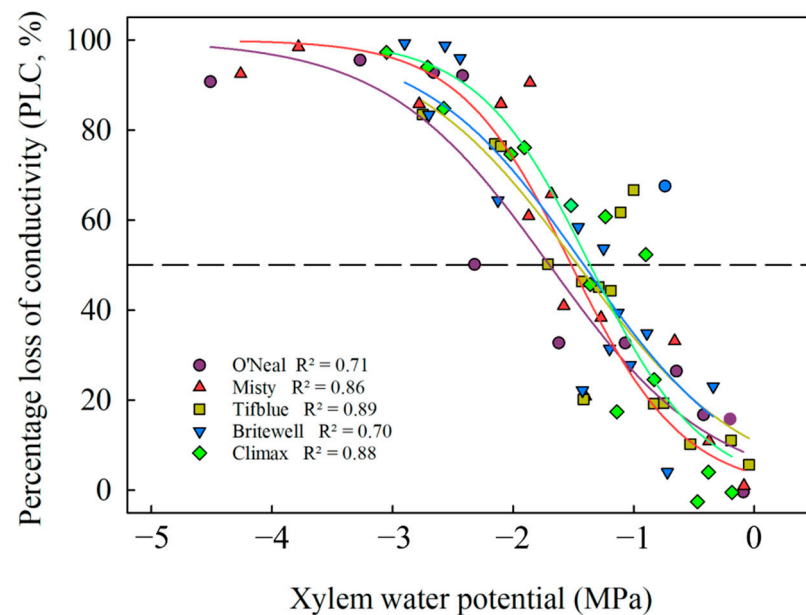


Figure 1. Xylem embolism vulnerability curves of five blueberry cultivar stems. The curves were established with the bench dehydration method. Different symbols and regression lines with the same color represent five blueberry cultivars. The horizontal dashed line gives 50% loss of hydraulic conductivity occurring in xylem.

Significant differences in hydraulic conductivities between two blueberry species were found, with SHB having significantly lower K_H and K_S than REB (Figure 2a; Table S1). The K_H of the five blueberry cultivars in order of strength to weakness was Britewell > Climax > Tifblue > Misty > O'Neal. A similar trend was found in K_S for five cultivars, except that Tifblue showed the highest K_S ($1.86 \pm 0.24 \text{ kg s}^{-1} \text{ MPa}^{-1} \text{ m}^{-1}$) (Figure 2b; Table S1).

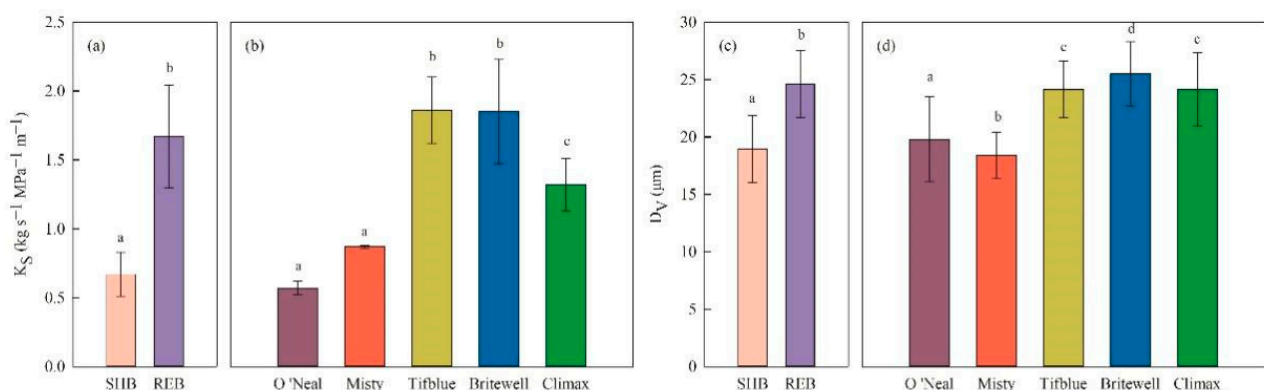


Figure 2. Cont.

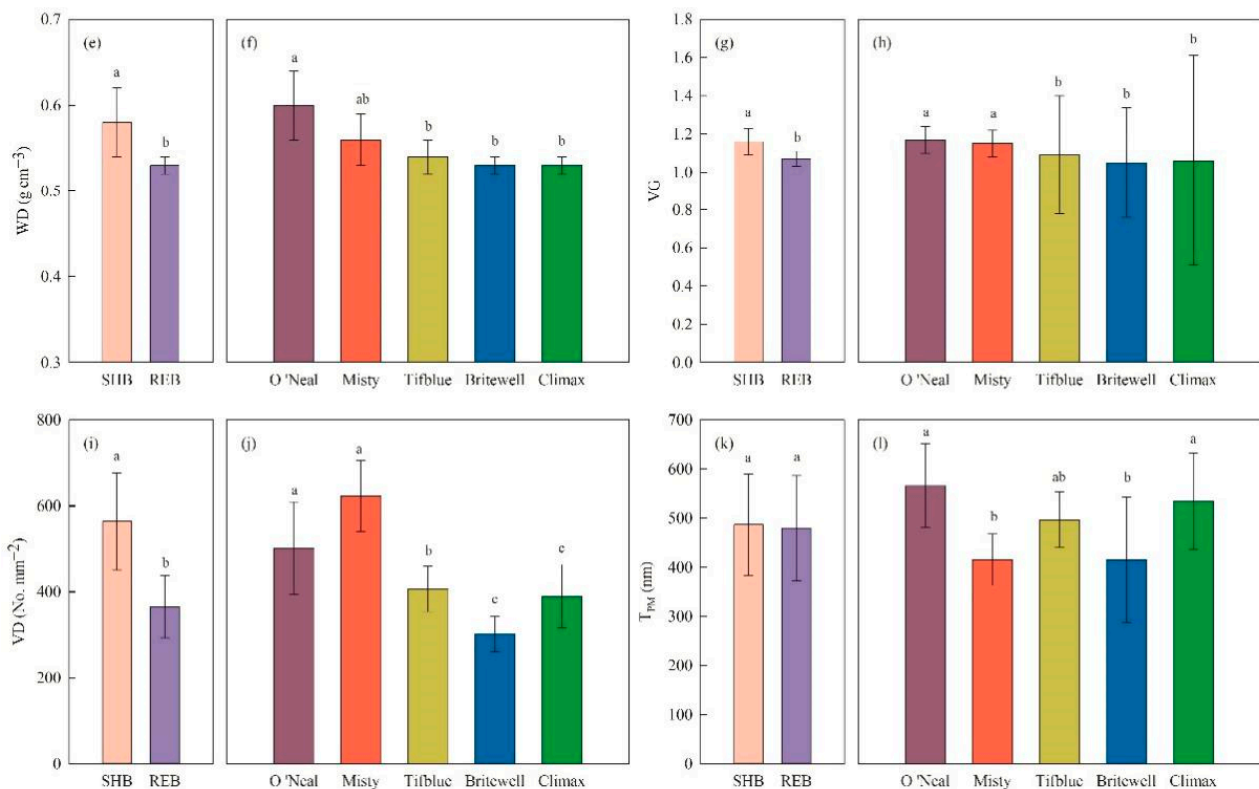


Figure 2. Comparison of sapwood hydraulic conductivity (K_s , (a,b)), vessel diameter (D_v , (c,d)), wood density (WD, (e,f)), vessel-grouping index (VG, (g,h)), vessel density (VD, (i,j)), and pit membrane thickness (T_{PM} , (k,l)) in five cultivars belonging to southern highbush and rabbiteye blueberries. SHB data represent the means of two southern highbush blueberry cultivars, including O'Neal and Misty, and REB data represent the means of three rabbiteye blueberry cultivars, including Britewell, Climax, and Tifblue. Different lowercase letters indicate statistically significant differences in traits among cultivars ($p < 0.05$), while same lowercase letters represent no significant differences in traits among cultivars ($p > 0.05$).

3.2. Differences in Xylem Anatomical Traits

Anatomical observations showed that the xylem structure of five blueberry cultivars varied at different scales. Vessel diameter (D_v) of SHB ($18.95 \pm 2.91 \mu\text{m}$) was significantly smaller than that of REB ($24.61 \pm 2.95 \mu\text{m}$) ($p < 0.01$; Table S1; Figure 2c). However, vessel density (VD), wood density (WD), conduct wall reinforcement (CWR), and vessel-grouping index (VG) were all greater in the SHB than in the REB (Figure 2e–h; Table S1).

All five blueberry cultivars showed bordered pits. Although pit density (PD) was significantly greater in SHB than in REB, the single pit aperture area (A_{SP}) was significantly smaller than in REB (Table S1). Similarly, the total area of inner pit aperture (A_{PA}) of SHB ($0.14 \pm 0.04 \mu\text{m}^2$) was significantly smaller than that of REB ($0.34 \pm 0.04 \mu\text{m}^2$) ($p = 0.02$; Table S1). Besides, two types of pit membranes in inter-vessel pits or vessel-tracheid pits were found in all five cultivars. One type only showed a straight and homogeneous outlook lying in the middle of a pit (Figure 3a,b), while the other type showed pseudo-tori with torus-like thickenings arching in the middle of a pit membrane (Figure 3a,c). The thickness of the pit membrane (without pseudo-tori) in SHB ($486.59 \pm 102.64 \text{ nm}$) was slightly higher than that in REB ($479.84 \pm 106.76 \text{ nm}$), but no significant difference between the two species was found ($p = 0.92$, Table S1). The thickness of the pseudo-tori pit membranes was not measured due to the irregular shape of the pseudo-tori.

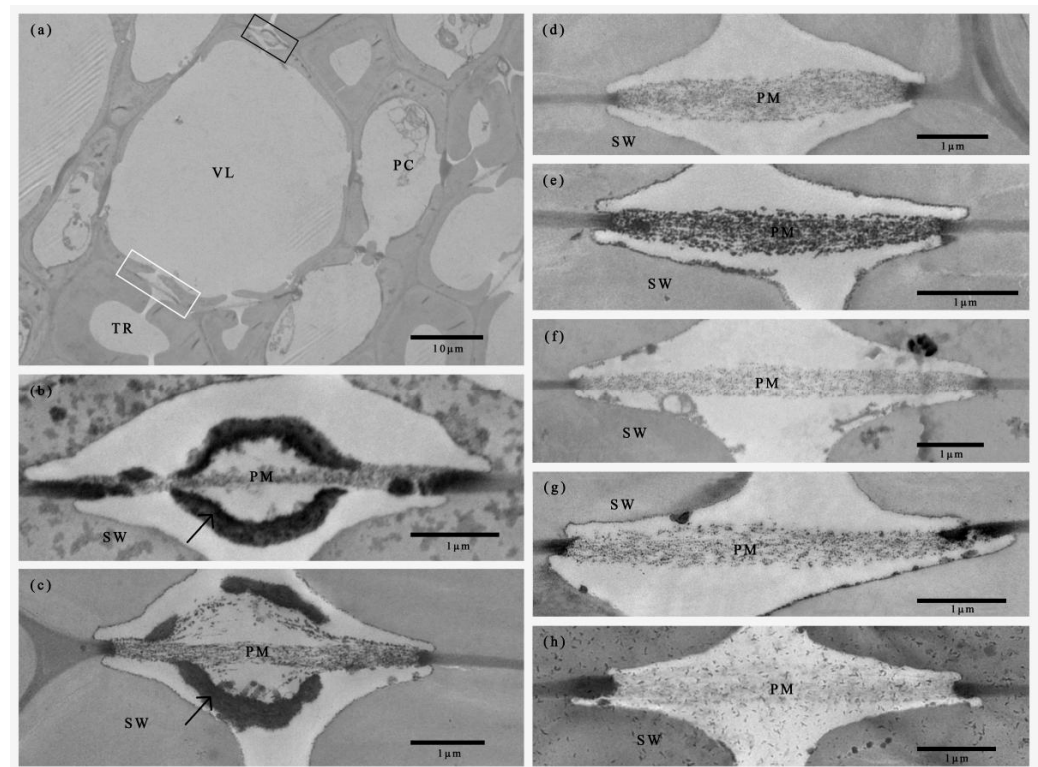


Figure 3. Transmission electron microscope images of stem xylem of Misty (a,e), O’Neal (b,d), Tifblue (c,f), Britewell (g), and Climax (h). Both homogenous pit membrane (a,d–h) and pseudo-tori pit membrane (a–c) are shown in cross-sections of stem xylem. The white and black box shows the homogenous pit membrane and the pseudo-torus pit membrane, respectively. The black arrow points to the pseudo-torus arching over the pit membrane. VL = vessel lumen, TR = tracheid, PC = parenchyma cell, SW = secondary wall, PM = pit membrane.

3.3. The Relationships between Functional and Anatomical Traits

Most xylem functional and anatomical traits of five blueberry cultivars were significantly correlated (Table 2). Both K_H and K_S were positively related to D_V and A_{PA} (K_S and A_{PA} were marginally correlated with $p = 0.07$) and negatively correlated with CWR, WD, and VG (Table 2). Xylem embolism resistance ability (represented as P_{50}) decreased with increasing D_V , but the significance of the relationship between these two was not strong ($p = 0.085$, Table 2). When WD, CWR, and VG increased, the resistance to embolism in xylem was subsequently enhanced (Table 2, Figure 4a,b). Besides, P_{50} was weakly related to PD and A_{SP} (Table 2), but highly linked to A_{PA} ($p = 0.007$, Figure 4c). However, pit membrane thickness (T_{PM}) in the xylem of five cultivars showed no significant relationships with both P_{50} and hydraulic conductivities (Table 2).

Moreover, P_{50} showed positive relations to K_H and K_S , although only P_{50} and K_H correlated significantly ($p = 0.042$, Table 2). D_V was negatively related to VD, CWR, and VG, while CWR was positively related to WD and VG (Table 2). VD was positively related to PD, but negatively linked to A_{SP} . A_{PA} was negatively linked to WD and VG, while WD and VG were positively related. T_{PM} showed no significant relationships to all other anatomical traits (Table 2).

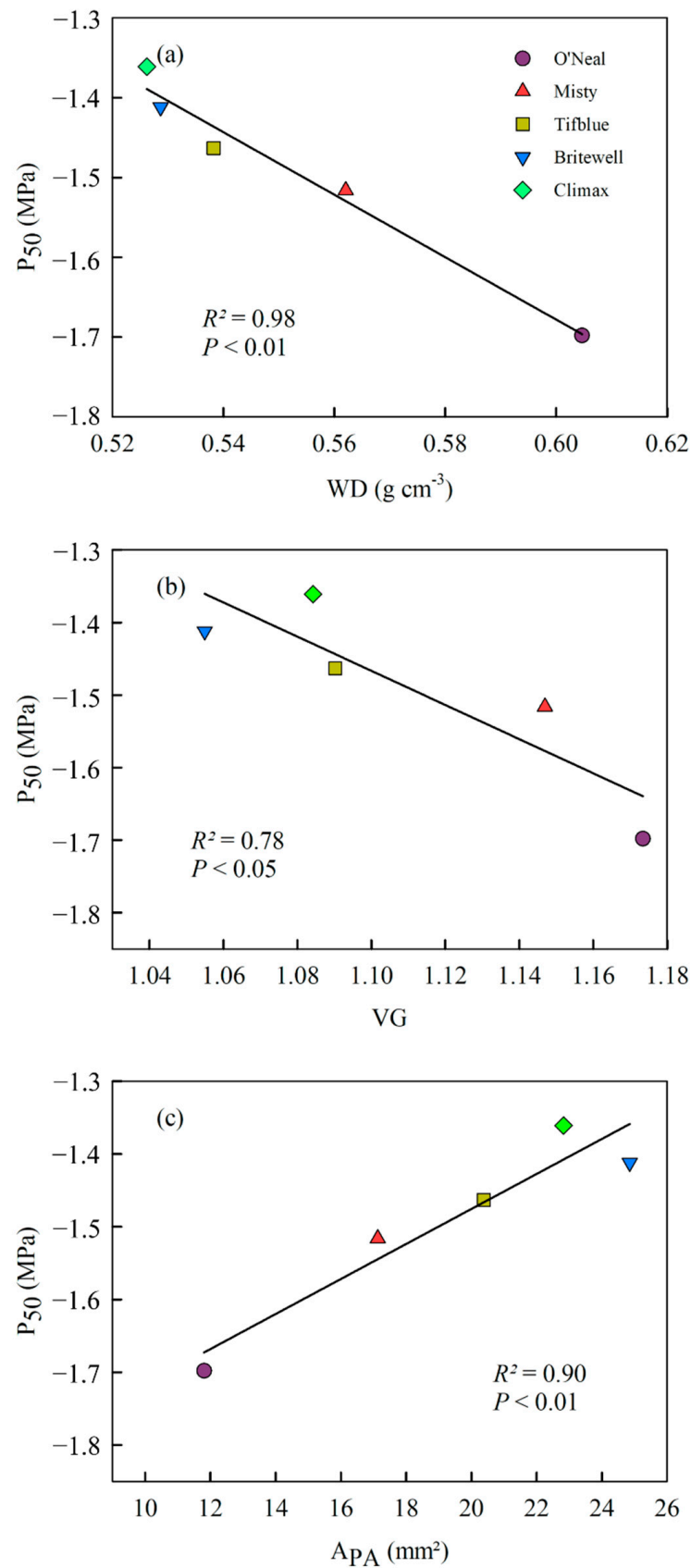


Figure 4. Linear analysis of P_{50} and wood density (WD, (a)), vessel-grouping index (VG, (b)), and total pit aperture area per vessel wall area (A_{PA} , (c)) for five blueberry cultivars. Different symbols with different colors represent five cultivars.

Table 2. Correlation matrix showing ‘R’ values between traits.

| | P ₅₀ | K _H | K _S | D _V | VD | CWR | WD | VG | PD | A _{SP} | A _{PA} | T _{PM} |
|-----------------|-----------------|-----------------|----------------|----------------|----------------|-----------------|-----------------|----------------|--------|-----------------|-----------------|-----------------|
| P ₅₀ | 1 | | | | | | | | | | | |
| K _H | 0.828 * | 1 | | | | | | | | | | |
| K _S | 0.746 | 0.853 * | 1 | | | | | | | | | |
| D _V | 0.720 | 0.948 ** | 0.884 * | 1 | | | | | | | | |
| VD | −0.564 | −0.912 * | −0.776 | −0.967 ** | 1 | | | | | | | |
| CWR | −0.848 * | −0.956 ** | −0.918 * | −0.975 ** | 0.891 | 1 | | | | | | |
| WD | −0.986 ** | −0.867 * | −0.845 * | −0.786 | 0.631 | 0.900 * | 1 | | | | | |
| VG | −0.928 * | −0.969 ** | −0.848 * | −0.920 * | 0.831 * | 0.972 ** | 0.875 ** | 1 | | | | |
| PD | −0.622 | −0.915 * | −0.630 | −0.804 | 0.861 * | 0.762 | 0.644 | 0.809 * | 1 | | | |
| A _{SP} | 0.544 | 0.740 | 0.530 | 0.846 * | −0.852 * | −0.793 | −0.55 | −0.752 | −0.626 | 1 | | |
| A _{PA} | 0.951 ** | 0.944 ** | 0.855 | 0.840 * | −0.735 | −0.919 | −0.922 ** | −0.971 ** | −0.801 | 0.576 | 1 | |
| T _{PM} | −0.268 | 0.048 | −0.383 | 0.083 | −0.283 | 0.070 | 0.500 | 0.048 | −0.293 | 0.475 | −0.206 | 1 |

For definitions of traits see Table 1. Values in bold show a statistical significance with * representing $p < 0.05$ and ** representing $p < 0.01$.

4. Discussion

The xylem vulnerability curves of five blueberry cultivars showed similar “S” shapes with the curve reported in Bluecrop, a northern highbush blueberry cultivar [19], which suggests that xylem embolism may occur in a similar pattern under drought stress in different blueberry species. However, Bluecrop showed a P₅₀ of −1.4 MPa [19], which is close to that of REB (−1.41 MPa) but higher than that of SHB (−1.61 MPa), although a statistical significance is lacking due to the limit P₅₀ values. Besides, lower P₁₂ and P₈₈ values were found in SHB than REB, suggesting that SHB may have a more embolism-resistant xylem than REB since SHB could withstand higher hydraulic conductivity and function better at a certain drought stress than SHB. This relative drought-resistant xylem in SHB, together with their low requirements for chilling [2], may contribute to the success of their cultivation in warm and dry regions.

Contrary to the high drought resistance for stems of SHB, leaves of SHB were reported to be less drought-resistant than leaves of REB [28]. Leaves of Britewell and Tifblue showed better ability in water control than Misty and O’Neal based on a comprehensive evaluation of five characteristic anatomical traits, including stomatal density, stomatal length, epidermis thickness, cuticle thickness, and the ratio of palisade tissue to spongy tissue [28]. However, it is not uncommon for different organs of a certain species to show different drought tolerances [29]. Distal organs, e.g., leaves, are prone to be more embolism-vulnerable than proximal organs, e.g., stems; this is called the hydraulic vulnerability segmentation hypothesis [30]. However, this hypothesis is not universal [31–33], and different species may exhibit contrasting trends of embolism resistance differences between leaves and stems [29,34]. Further studies on hydraulic properties in blueberry leaves, such as leaf hydraulic conductivity and leaf vulnerability curve, may help to better clarify the discrepancy in embolism resistance between blueberry organs.

The significant differences in anatomical traits of two blueberry xylems (Figure 2) may contribute to their drought resistance difference since most of the anatomical traits are highly related to functional traits in xylems of five cultivars (Table 2; Figure 4). Wider vessels found in REB than SHB largely determine the higher K_S and K_H of the REB xylem (Table 2; Figure 2) since the conductivity is positively linked to the fourth power of the conduit diameter according to the Hagen–Poiseuille equation [35]. The highly conductive xylems also show high P₅₀ values in five cultivars, suggesting a trade-off between high efficiency and high safety for water transport in blueberry xylems (Table 2). This trade-off relationship has been found in many angiosperm species [36–39] and may be confirmed by the negative correlations between hydraulic traits (K_H and K_S) and CWR, WD, and VG (Table 2).

The conduit wall reinforcement (CWR), representing the ratio of vessel diameter and cell wall thickness, is closely related to the xylem embolism resistance [40,41]. Compared with REB xylem, higher CWR values in the SHB xylem correspond to its smaller vessel diameter and lower P₅₀ (Table S1, Table 2), suggesting a less conductive but safer xylem of SHB than REB. Besides, wood density (WD) also influences xylem embolism resistance

by affecting the mechanical strength of xylem [40,42–44], which explains the negative relationship between WD and P_{50} , and therefore, the negative relationship between WD and K_S .

The negative relationship between vessel-grouping index (VG) and P_{50} in five blueberry cultivars supports the early hypothesis proposed by Carlquist [45] that a high degree of vessel connectivity is found in xeric-adapted species. Grouping of vessels provides alternate functional vessels in case one or several vessels in a group are failed for water transport due to embolism [45,46] and thus contributes to drought resistance [47]. Therefore, SHB xylem with higher VG may have a lower risk of dysfunction under drought stress than REB xylem.

According to the “rare pit” hypothesis [48,49], the high vessel connectivity also increases the likelihood of embolism spreading through rare leaking pits on adjacent vessel walls and therefore leads to increased embolism vulnerability [50,51]. Experimental evidence shows that vessels with less total pit area, pit number, and smaller pit aperture are less embolized [15,24,47,52]. However, weak relationships of P_{50} -PD and P_{50} - A_{SP} are found in five blueberry cultivars, which indicates a weak link between xylem embolism resistance and the geometry of pits measured in a single vessel. Instead, A_{PA} , reflecting the network of vessels in xylem and strongly linked to P_{50} , may show a positive effect on xylem embolism resistance. A lower A_{PA} value indicates less total pit aperture area on the entire lateral vessel walls adjacent to other vessels and, therefore, leads to lower hydraulic conductivity and as well as higher water transport safety.

However, an unexpected negative, instead of positive, correlation between A_{PA} and VG was found in five cultivars (Table 2), considering that both traits represent a connectivity degree of the vessels in xylem. Nevertheless, A_{PA} and VG may not be intrinsically related because A_{PA} is calculated based on multiple parameters, such as vessel diameter, vessel length, and pit aperture density, while VG is obtained from a cross-section representing the number of grouped vessels. Therefore, both traits may explain the vessel connectivity from different perspectives. More attention is needed to clarify the functional reasons for the variation of the vessel connectivity in the xylem of angiosperms [47].

Moreover, the thickness of the pit membrane (T_{PM}) is regarded as a good indicator of xylem drought resistance due to its highly negative relation to P_{50} values based on studies among various species [17,53,54]. Pit membrane consists of layers of microfibrils, and numerous nanopores woven by these microfibrils create complex pathways for water transport and embolism (or air bubbles) spreading in neighboring vessels. Thick pit membranes represent longer pathways and increase the chance of air bubbles being snapped into small nanobubbles, which largely reduces embolism spreading and promotes embolism resistance [55]. Besides, thick pit membrane is found to show small pores, which represents narrow pathways for air bubbles [54]. However, T_{PM} is not related to P_{50} in five blueberry cultivars (Table 2), and both SHB and REB show similar T_{PM} (Table S1). This may be due to the limited measurements of T_{PM} for each cultivar, but perhaps more importantly, due to the pseudo-tori pits found in all cultivars, which are also reported in other Ericaceae species [54]. These pits with pseudo-tori structure are not included in the statistical analysis of the T_{PM} - P_{50} relation since the T_{PM} measurements become difficult due to the amorphous shape of pseudo-tori. However, the function of pseudo-tori is unclear and may link to the function of plasmodesmata during the differentiation of tracheary elements [56]. Further research could focus on the distribution and development of pseudo-tori pits in the xylem of blueberries.

5. Conclusions

Investigations on the xylem hydraulic properties of stems of five blueberry cultivars provide new insights into understanding the stem embolism resistance and drought tolerance of blueberries. Southern highbush blueberry cultivars show relatively higher embolism resistance but less conductive xylem in stems than rabbiteye blueberry cultivars, which may contribute to the expanding growing area of southern highbush blueberries in

warm and arid regions worldwide. Besides, anatomical and hydraulic traits of stem xylem in five blueberry cultivars are highly related, but further studies focusing on hydraulic properties of leave and roots of blueberries are needed to link the water transport system in a whole plant. Clarifying the potential hydraulic relations of different organs could provide a comprehensive view of drought adaptability variations of different blueberry cultivars, which will build a solid basis for cultivation and management in blueberry industries.

Supplementary Materials: The following supporting information can be downloaded at: <https://www.mdpi.com/article/10.3390/agronomy12051244/s1>, Table S1: Xylem functional and anatomical data of five blueberry cultivars.

Author Contributions: Conceptualization, Y.Z.; methodology, Y.Z. and J.-B.L.; software, J.-B.L.; formal analysis, J.-B.L.; writing—original draft preparation, J.-B.L.; writing—review and editing, Y.Z., J.-B.L. and X.-X.Z.; supervision, Y.Z.; funding acquisition, Y.Z. All authors have read and agreed to the published version of the manuscript.

Funding: This research was funded by the National Natural Science Foundation of China (32001105).

Data Availability Statement: Any data and codes used in this study are available upon request from the corresponding author.

Acknowledgments: We would like to thank the staff from the Huiwang Meiling Blueberry Plantation for their assistance in plant collection.

Conflicts of Interest: The authors declare no conflict of interest.

References

1. Lobos, G.A.; Hancock, J.F. Breeding blueberries for a changing global environment: A review. *Front. Plant Sci.* **2015**, *6*, 782. [CrossRef] [PubMed]
2. Retamales, J.B.; Hancock, J.F. *Blueberries*; CABI Publishing: Wallingford, UK, 2012; pp. 1–2.
3. Erb, W.A. Improved drought tolerance and root development as components of a scheme to breed blueberries for mineral soil adaptability. *Euphytica* **1993**, *70*, 9–16. [CrossRef]
4. Gui, L.X.; Lu, S.S.; Chen, Q.; Xiao, J.X. iTRAQ-based proteomic analysis reveals positive impacts of arbuscular mycorrhizal fungi inoculation on photosynthesis and drought tolerance in blueberry. *Trees* **2020**, *35*, 81–92. [CrossRef]
5. Mingau, M.; Perrier, C.; Améglio, T. Evidence of drought-sensitive periods from flowering to maturity on highbush blueberry. *Sci. Hortic.* **2001**, *89*, 23–40. [CrossRef]
6. Chen, Y.Y.; Pahadi, P.; Calderwood, L.; Annis, S.; Drummond, F.; Zhang, Y.J. Will Climate Warming Alter Biotic Stresses in Wild Lowbush Blueberries? *Agronomy* **2022**, *12*, 371. [CrossRef]
7. Balboa, K.; Ballesteros, G.I.; Molina-Montenegro, M.A. Integration of Physiological and Molecular Traits Would Help to Improve the Insights of Drought Resistance in Highbush Blueberry Cultivars. *Plants* **2020**, *9*, 1457. [CrossRef]
8. Molnar, S.; Clapa, D.; Mitre, V. Response of the Five Highbush Blueberry Cultivars to In Vitro Induced Drought Stress by Polyethylene Glycol. *Agronomy* **2022**, *12*, 732. [CrossRef]
9. Cameron, J.S.; Brun, C.A.; Hartley, C.A. The influence of soil moisture stress on the growth and gas exchange characteristics of young highbush blueberry plants (*Vaccinium corymbosum* L.). *Acta Hortic.* **1989**, *241*, 254–259. [CrossRef]
10. Rho, H.; Yu, D.J.; Kim, S.J.; Lee, H.J. Limitation factors for photosynthesis in ‘Bluecrop’ highbush blueberry (*Vaccinium corymbosum*) leaves in response to moderate water stress. *J. Plant Biol.* **2012**, *55*, 450–457. [CrossRef]
11. Chen, X.M.; Qiu, L.L.; Guo, H.P.; Wang, Y.; Yuan, H.W.; Yan, D.L.; Zheng, B.S. Spermidine induces physiological and biochemical changes in southern highbush blueberry under drought stress. *Braz. J. Bot.* **2017**, *40*, 841–851. [CrossRef]
12. Awad, H.; Barigah, T.; Badel, E.; Cochard, H.; Herbette, S. Poplar vulnerability to xylem cavitation acclimates to drier soil conditions. *Physiol. Plant* **2010**, *139*, 280–288. [CrossRef] [PubMed]
13. Skelton, R.P.; West, A.G.; Dawson, T.E. Predicting plant vulnerability to drought in biodiverse regions using functional traits. *Proc. Natl. Acad. Sci. USA* **2015**, *112*, 5744–5749. [CrossRef] [PubMed]
14. Tyree, M.T.; Sperry, J.S. Vulnerability of Xylem to Cavitation and Embolism. *Annu. Rev. Plant Phys. Mol. Biol.* **1989**, *40*, 19–38. [CrossRef]
15. Hacke, U.G.; Sperry, J.S.; Wheeler, J.K.; Laura, C. Scaling of angiosperm xylem structure with safety and efficiency. *Tree Physiol.* **2006**, *26*, 689–701. [CrossRef]
16. Hacke, U.G.; Sperry, J.S.; Field, T.S.; Sano, Y.; Sikkema, E.H.; Pittermann, J. Water transport in vesselless angiosperms: Conducting efficiency and cavitation safety. *Int. J. Plant Sci.* **2007**, *168*, 1113–1126. [CrossRef]
17. Li, S.; Lens, F.; Espino, S.; Karimi, Z.; Klepsch, M.; Schenk, H.J.; Schmitt, M.; Schuldt, B.; Jansen, S. Intervessel pit membrane thickness as a key determinant of embolism resistance in angiosperm xylem. *IAWA J.* **2016**, *37*, 152–171. [CrossRef]

18. Lobo, A.; Torres-Ruiz, J.M.; Burlett, R.; Lemaire, C.; Parise, C.; Francioni, C.; Truffaut, L.; Tomášková, I.; Hansen, J.K.; Kjær, E.D.; et al. Assessing inter- and intraspecific variability of xylem vulnerability to embolism in oaks. *For. Ecol. Manag.* **2018**, *424*, 53–61. [\[CrossRef\]](#)
19. Améglio, T.; Roux, X.L.E.; Mingeau, M.; Perrier, C. Water relations of highbush blueberry under drought conditions. *Acta Hort.* **2000**, *537*, 273–278. [\[CrossRef\]](#)
20. Sperry, J.S.; Donnelly, J.R.; Tyree, M.T. A method for measuring hydraulic conductivity and embolism in xylem. *Plant Cell Environ.* **1988**, *11*, 35–40. [\[CrossRef\]](#)
21. Zimmermann, M.H.; Jeje, A.A. Vessel-length distribution in stems of some American woody plants. *Can. J. Bot.* **1981**, *59*, 1882–1892. [\[CrossRef\]](#)
22. Domec, J.C.; Gartner, B.L. Cavitation and water storage capacity in bole xylem segments of mature and young Douglas-fir trees. *Trees* **2001**, *15*, 204–214. [\[CrossRef\]](#)
23. Scholz, A.; Klepsch, M.; Karimi, Z.; Jansen, S. How to quantify conduits in wood? *Front. Plant Sci.* **2013**, *4*, 56. [\[CrossRef\]](#)
24. Wheeler, J.K.; Sperry, J.S.; Hacke, U.G.; Hoang, H. Inter-vessel pitting and cavitation in woody Rosaceae and other vesselled plants: A basis for a safety versus efficiency trade-off in xylem transport. *Plant Cell Environ.* **2005**, *28*, 800–812. [\[CrossRef\]](#)
25. Sperry, J.S.; Hacke, U.G.; Wheeler, J.K. Comparative analysis of end wall resistivity in xylem conduits. *Plant Cell Environ.* **2005**, *28*, 456–465. [\[CrossRef\]](#)
26. Kaack, L.; Altaner, C.M.; Carmesin, C.; Diaz, A.; Holler, M.; Kranz, C.; Neusser, G.; Odstřil, M.; Schenk, H.J.; Schmidt, V.; et al. Function and three dimensional structure of intervessel pit membranes in angiosperms: A review. *IAWA J.* **2019**, *40*, 673–702. [\[CrossRef\]](#)
27. Kotowska, M.M.; Thom, R.; Zhang, Y.; Schenk, H.J.; Jansen, S. Within-tree variability and sample storage effects of bordered pit membranes in xylem of *Acer pseudoplatanus*. *Trees* **2020**, *34*, 61–71. [\[CrossRef\]](#)
28. Tang, J.W.; Wu, S.Z.; Liang, W.B.; Li, J.H.; Bai, W.F.; Yu, L.; Nie, D.L. Leaf structure characteristics and drought resistance of blueberry in Hunan Province. *Nonwood For. Res.* **2017**, *35*, 90–98. (In Chinese) [\[CrossRef\]](#)
29. Wu, M.; Zhang, Y.; Oya, T.; Marcati, C.R.; Pereira, L.; Jansen, S. Root xylem in three woody angiosperm species is not more vulnerable to embolism than stem xylem. *Plant Soil* **2020**, *450*, 479–495. [\[CrossRef\]](#)
30. Tyree, M.T.; Ewers, F.W. The hydraulic architecture of trees and other woody plants. *New Phytol.* **1991**, *119*, 345–360. [\[CrossRef\]](#)
31. Charrier, G.; Torres-Ruiz, J.M.; Badel, E.; Burlett, R.; Choat, B.; Cochard, H.; Delmas, C.E.; Domec, J.C.; Jansen, S.; King, A.; et al. Evidence for Hydraulic Vulnerability Segmentation and Lack of Xylem Refilling under Tension. *Plant Physiol.* **2016**, *172*, 1657–1668. [\[CrossRef\]](#)
32. Rodriguez-Dominguez, C.M.; Carins Murphy, M.R.; Lucani, C.; Brodribb, T.J. Mapping xylem failure in disparate organs of whole plants reveals extreme resistance in olive roots. *New Phytol.* **2018**, *218*, 1025–1035. [\[CrossRef\]](#) [\[PubMed\]](#)
33. Skelton, R.P.; Brodribb, T.J.; Choat, B. Casting light on xylem vulnerability in an herbaceous species reveals a lack of segmentation. *New Phytol.* **2017**, *214*, 561–569. [\[CrossRef\]](#)
34. Klepsch, M.; Zhang, Y.; Kotowska, M.M.; Lamarque, L.J.; Nolf, M.; Schuldt, B.; Torres-Ruiz, J.M.; Qin, D.W.; Choat, B.; Delzon, S.; et al. Is xylem of angiosperm leaves less resistant to embolism than branches? Insights from micro CT, hydraulics, and anatomy. *J. Exp. Bot.* **2018**, *69*, 5611–5623. [\[CrossRef\]](#) [\[PubMed\]](#)
35. Tyree, M.T.; Zimmermann, M.H. *Xylem Structure and the Ascent of Sap*, 2nd ed.; Springer: Berlin, Germany, 2002; pp. 45–56.
36. Hargrave, K.R.; Kolb, K.J.; Ewers, F.W.; Davis, S.D. Conduit diameter and drought induced embolism in *Salvia mellifera* Greene (Labiatae). *New Phytol.* **1994**, *126*, 695–705. [\[CrossRef\]](#)
37. Cai, J.; Tyree, M.T. The impact of vessel size on vulnerability curves: Data and models for within-species variability in saplings of aspen, *Populus tremuloides* Michx. *Plant Cell Environ.* **2010**, *33*, 1059–1069. [\[CrossRef\]](#)
38. Gleason, S.M.; Westoby, M.; Jansen, S.; Choat, B.; Hacke, U.G.; Pratt, R.B.; Bhaskar, R.; Brodribb, T.J.; Bucci, S.J.; Cao, K.F.; et al. Weak tradeoff between xylem safety and xylem-specific hydraulic efficiency across the world's woody plant species. *New Phytol.* **2016**, *209*, 123–136. [\[CrossRef\]](#)
39. Schumann, K.; Leuschner, C.; Schuldt, B. Xylem hydraulic safety and efficiency in relation to leaf and wood traits in three temperate *Acer* species differing in habitat preferences. *Trees* **2019**, *33*, 1475–1490. [\[CrossRef\]](#)
40. Hacke, U.G.; Sperry, J.S.; Pockman, W.P.; Davis, S.D.; MacCulloh, K.A. Trends in wood density and structure are linked to prevention of xylem implosion by negative pressure. *Oecologia* **2001**, *126*, 457–461. [\[CrossRef\]](#)
41. Cochard, H.; Barigah, S.T.; Kleinhentz, M.; Eshel, A. Is xylem cavitation resistance a relevant criterion for screening drought resistance among *Prunus* species? *J. Plant Physiol.* **2008**, *165*, 976–982. [\[CrossRef\]](#)
42. Jansen, S.; Choat, B.; Pletsers, A. Morphological variation of intervessel pit membranes and implications to xylem function in angiosperms. *Am. J. Bot.* **2009**, *96*, 409–419. [\[CrossRef\]](#)
43. Plavcová, L.; Hacke, U.G.; Sperry, J.S. Linking irradiance-induced changes in pit membrane ultrastructure with xylem vulnerability to cavitation. *Plant Cell Environ.* **2011**, *34*, 501–513. [\[CrossRef\]](#) [\[PubMed\]](#)
44. Jacobsen, A.L.; Ewers, F.W.; Pratt, R.B.; Paddock, W.A., III; Davis, S.D. Do xylem fibers affect vessel cavitation resistance? *Plant Physiol.* **2005**, *139*, 546–556. [\[CrossRef\]](#) [\[PubMed\]](#)
45. Carlquist, S. Vessel grouping in dicotyledon wood. *Aliso* **1984**, *10*, 505–525. [\[CrossRef\]](#)
46. Carlquist, S. Xylem heterochrony: An unappreciated key to angiosperm origin and diversifications. *Bot. J. Linn. Soc.* **2009**, *161*, 26–65. [\[CrossRef\]](#)

47. Lens, F.; Sperry, J.S.; Christman, M.A.; Choat, B.; Rabaey, D.; Jansen, S. Testing hypotheses that link wood anatomy to cavitation resistance and hydraulic conductivity in the genus *Acer*. *New Phytol.* **2011**, *190*, 709–723. [[CrossRef](#)] [[PubMed](#)]
48. Christman, M.A.; Sperry, J.S.; Adler, F.R. Testing the ‘rare pit’ hypothesis for xylem cavitation resistance in three species of *Acer*. *New Phytol.* **2009**, *182*, 664–674. [[CrossRef](#)]
49. Christman, M.A.; Sperry, J.S.; Smith, D.D. Rare pits, large vessels and extreme vulnerability to cavitation in a ring-porous tree species. *New Phytol.* **2012**, *193*, 713–720. [[CrossRef](#)]
50. Loepfe, L.; Martínez-Vilalta, J.; Pinol, J.; Mencuccini, M. The relevance of xylem network structure for plant hydraulic efficiency and safety. *J. Theor. Biol.* **2007**, *247*, 788–803. [[CrossRef](#)]
51. Martínez-Vilalta, J.; Mencuccini, M.; Alvarez, X.; Camacho, J.; Loepfe, L.; Piñol, J. Spatial distribution and packing of xylem conduits. *Am. J. Bot.* **2012**, *99*, 1189–1196. [[CrossRef](#)]
52. Sperry, J.S.; Hacke, U.G.; Pittermann, J. Size and function in conifer tracheids and angiosperm vessels. *Am. J. Bot.* **2006**, *93*, 1490–1500. [[CrossRef](#)]
53. Levionnois, S.; Jansen, S.; Wandji, R.T.; Beauchêne, J.; Ziegler, C.; Coste, S.; Stahl, C.L.; Delzon, S.; Authier, L.; Heuret, P. Linking drought-induced xylem embolism resistance to wood anatomical traits in Neotropical trees. *New Phytol.* **2020**, *229*, 1179–1823. [[CrossRef](#)] [[PubMed](#)]
54. Kaack, L.; Weber, M.; Isasa, E.; Karimi, Z.; Li, S.; Pereira, L.; Trabi, C.L.; Zhang, Y.; Schenk, H.J.; Schuldt, B.; et al. Pore constrictions in intervessel pit membranes provide a mechanistic explanation for xylem embolism resistance in angiosperms. *New Phytol.* **2021**, *230*, 1829–1843. [[CrossRef](#)] [[PubMed](#)]
55. Jansen, S.; Klepsch, M.; Li, S.; Kotowska, M.M.; Schiele, S.; Zhang, Y.; Schenk, H.J. Challenges in understanding air-seeding in angiosperm xylem. *Acta Hortic.* **2018**, *1222*, 13–20. [[CrossRef](#)]
56. Rabaey, D.; Lens, F.; Smets, E.; Jansen, S. The Micromorphology of Pit Membranes in Tracheary Elements of Ericales: New Records of Tori or Pseudo-tori? *Ann. Bot.* **2006**, *98*, 943–951. [[CrossRef](#)] [[PubMed](#)]